Infrared Low-Cloud Detection

Mark Hofstadter
JPL/Caltech

Andrew Heidinger
NOAA/NESDIS

28 October 1998

Submitted to the Journal of Atmospheric and Oceanic Technology

ABSTRACT

Traditional down-looking infrared techniques for the detection and study of clouds have difficulties when clouds are within approximately 200 mbar of the surface. This is because of the lack of thermal contrast between the surface and a low cloud. We present a technique that, using *a priori* knowledge of the total water column, allows a down-looking high spectral resolution infrared spectrometer to recognize when a significant fraction of its field-of-view contains optically thick clouds (low-altitude or not). This is done by comparing the observed opacity across optically thin water lines to the opacity expected for the known total water column. This technique can also improve retrievals of low-cloud height and amount in moist atmospheres. The Atmospheric Infrared Sounder (AIRS), to be flown as part of NASA's Earth Observing System, will be able to take full advantage of this technique in order to improve the accuracy of its temperature and moisture soundings, and to help improve our knowledge of the distribution and properties of low clouds. In particular, it is found that for a single cloud layer in a tropical atmosphere, the presence of a solid cloud deck can be recognized even within 50 mbar of the surface, while (compared to current techniques) the uncertainty in retrieved cloud altitude and coverage is substantially smaller for all low-cloud amounts.

remote sensing
IR Spectroscopy

1. Introduction

Orbiting infrared instruments are routinely used for global-scale retrieval of atmospheric and surface properties and for studying clouds. This information is crucial for weather forecasting, as well as climate and hydrological studies. If unrecognized clouds are present in an infrared field-of-view (FOV), this degrades the accuracy of retrieved profiles, since cloud properties may be mistakenly imposed on the atmosphere or surface. Traditional IR techniques for sounding in the presence of clouds use absolute radiance measurements. Smith (1968) discusses how this can be done with some *a priori* knowledge–such as surface temperature, while Chahine (1968, 1970) uses a relaxation technique that does not require external information. For these approaches to be effective, the difference between the clear column radiance and the cloudy column radiance must be greater than the uncertainty with which either can be determined by itself. As discussed by Wielicki and Coakley (1981), such techniques fail on low clouds. This is because low clouds are relatively warm, and the IR contrast between clear and cloudy columns is small.

This paper describes a new technique for IR cloud detection, which is a synthesis of the traditional IR approach and visible techniques (see O'Brien *et al.* 1997 for a recent discussion of the O_2 A-band technique). We use as our signal the depth of optically thin atmospheric lines, rather than the absolute radiance. Because the line depth, a differential quantity, is much less sensitive than the absolute radiance to most non-cloud parameters (such as surface temperature), the uncertainty associated with determining clear and cloudy line depths is relatively small. This allows the recognition of clouds with very little thermal contrast from the surface. For this technique to determine whether or not low clouds are present, the column abundance of the active species must be known. To retrieve cloud height and amount, it is necessary to have some measure of the vertical distribution of the species. We present an analysis of applying this technique to optically thin water vapor lines. Water is a good candidate for low-cloud detection because water is concentrated in the lowest levels of the atmosphere, and because microwave instruments can determine its total column abundance even in the presence of clouds. The Atmospheric Infrared Sounder (AIRS), an instrument to be flown on the Earth Observing System's PM-1 platform, is well suited to take advantage of this new approach by virtue of its relatively high spectral resolution ($\lambda/\Delta\lambda$ = 1200), and the fact that it will operate in conjunction with two microwave instruments (the Advanced Microwave Sounding Unit, AMSU, and the Humidity Sounder for Brazil, HSB). Modeling indicates AIRS can detect clouds in moist atmospheres even when they are within 50 mbar of the surface.

In the next section we show how this approach can, with minimal computational effort, be used to set a simple True/False flag for whether or not a cloud exists in a single infrared FOV. Section 3 then discusses how more sophisticated retrieval schemes can be used to determine cloud height and amount. The final section contains a summary. It should be emphasized that the water vapor method developed here is tailored to fill a region of parameter space the traditional methods miss, and it is only by using both techniques in parallel that we can improve our understanding of clouds, and improve the quality of IR atmospheric retrievals.

2. True/False Cloud Test

Figure 1 shows two simulated spectra for a downlooking infrared instrument in Earth orbit. In the main figure, there is a clear temperature offset between the clear and cloudy spectra in the window regions (800 to 1000 cm^{-1}, near 1100 cm^{-1}, and near 2500 cm^{-1}). A traditional inversion routine given the cloudy spectrum, however, could not reliably recognize it as such. It could instead be interpreted as a clear sky with a cooler surface, or a surface with low emissivity. The inset shows several optically thin water vapor lines, whose depth is determined primarily by the total number of vapor molecules in the optical path. Because the opaque cloud screens all water vapor below it from our view, the depth of these lines is smaller in the presence of clouds. This line depth (the brightness temperature difference between a clear frequency and a nearby line center frequency) is the primary observation used by the technique proposed here.

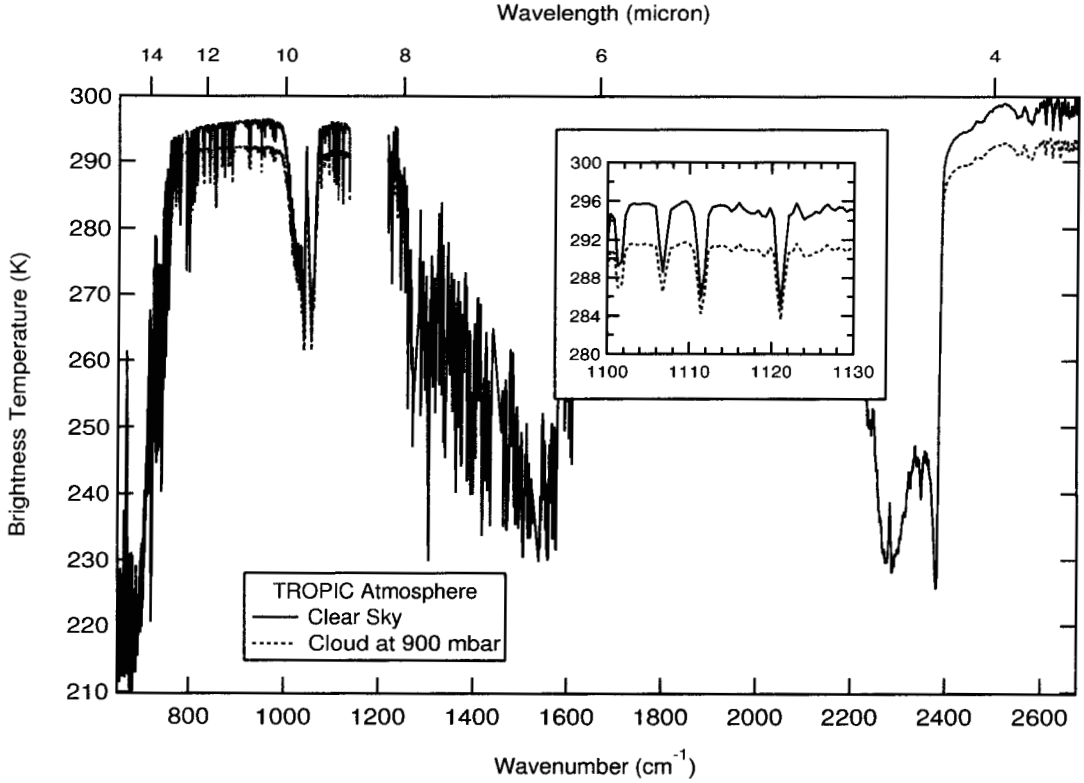

Figure 1: Simulated spectra for AIRS (see Aumann and Pagano 1994 for an instrument description.). Gaps in the spectra are frequencies not covered by AIRS detectors. The solid curve is for a clear sky, while the dashed has a blackbody cloud top at 900 mbar. The surface is at 300 K and it has an emissivity of 1.0. The absorption near 1000 cm^{-1} is due to ozone, and the sharp drop near 700 cm^{-1} is the CO_2 15 micron band. The broad depression at 1500 cm^{-1} is due to water vapor. So-called "window regions" exist between these strong absorption bands. The inset highlights some of the many water vapor lines present even in these windows. The McClatchey Tropical atmosphere is assumed (McClatchey *et al.* 1972).

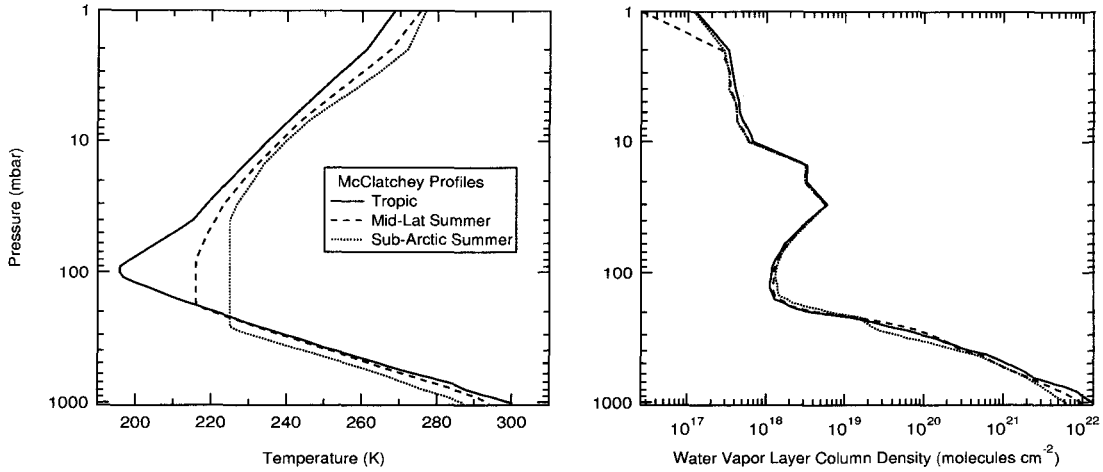

Figure 2: McClatchey temperature (left) and water vapor (right) profiles for the Tropic (solid), Mid-Latitude Summer (dashed), and Sub-Arctic Summer (dotted) cases. The water vapor curve shows the abundance within a finite layer whose base is at the indicated pressure level. The layer thickness is 25 mbar at pressures greater than 400 mbar, changing to 20 mbar steps between 400 and 200 mbar, and getting smaller at higher altitudes.

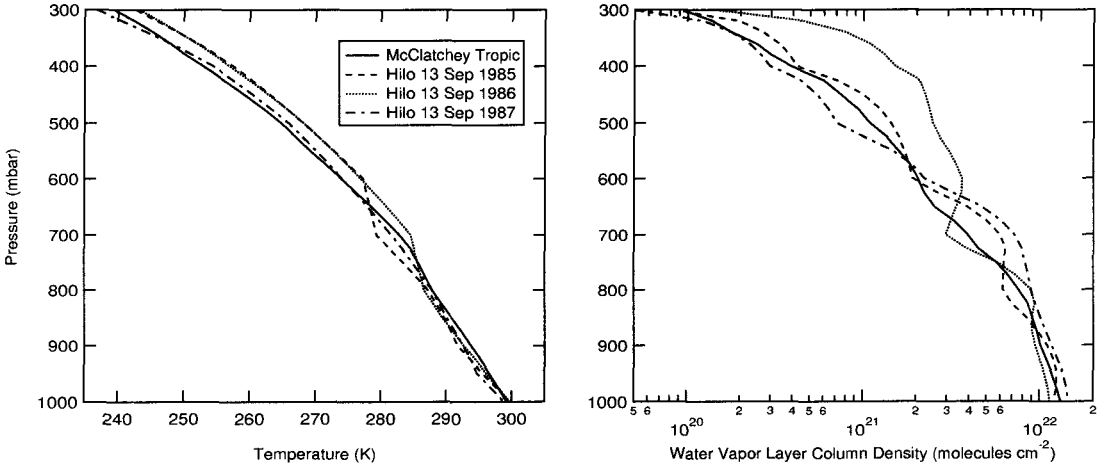

Figure 3: The McClatchey Tropical profile (solid) is compared to three radiosonde profiles from Hilo Hawaii, taken at 0 hours GMT (approximately 2 pm local time) on 13 September 1985 (dashed), 1986 (dotted), and 1987 (dot-dashed). Radiosonde data is used up to 300 mbar, above which the temperature is assumed isothermal and the water vapor abundance is set to zero. Note the change in scale between Figures 2 and 3, necessary to distinguish the radiosonde profiles from each other and from the Tropical case.

The line depth under clear-sky conditions is insensitive to such properties as surface temperature, surface emissivity, atmospheric temperature profile, and the vertical distribution of vapor within a column. This makes it an extremely sensitive indicator of clouds. Table I shows the total water column and calculated clear-sky line depths for the profiles shown in Figures 2 and 3, using a water line at 1121 cm^{-1}. (Note that the 1987 Hilo profile, which has the highest water abundance, does not have the largest line depth. This is due to enhanced line broadening, continuum absorption, and perhaps saturation effects at this vapor amount.) The far right column shows the line depth for the same profiles, but now the water vapor abundance at each altitude has been scaled by a constant factor to make the total column abundance match the McClatchey Tropical case. It can be

seen that all the scaled cases differ from the Tropical results by no more than 1.0 K This indicates that even with only a crude climatological-type knowledge of the temperature profile and water vapor scale height, the clear-sky line depth is known to within ~1 K if the total water column is known. The final four rows of Table I indicate the line depth sensitivity to knowledge of the total water column. For the Tropical case, variations of 20% change the line depth by less than 1 K.

Table I
Clear-Sky Line Depths at 1121 cm^{-1}

Atmosphere	Nominal H_2O Column ($g\ cm^{-2}$)	Line Depth (K) Nominal	Water Scaled to Tropical
Tropical	4.0	10.4	10.4
Mid-Lat Summer	2.8	8.4	9.5
Sub-Arctic Summer	2.0	8.0	10.2
Hilo, 13 Sep 1985	4.3	11.1	10.9
Hilo, 13 Sep 1986	4.5	11.8	11.4
Hilo, 13 Sep 1987	5.1	10.7	10.4
Tropical + 10%	4.4	10.6	
Tropical - 10%	3.6	10.1	
Tropical + 20%	4.8	10.8	
Tropical - 20%	3.2	9.7	

These results indicate that, if the total water column is known to within ~15%, the clear-sky line depth for the 1121 cm^{-1} weak water line is known to ~1 K. (The 15% level is the accuracy expected from the microwave instruments on board the EOS PM-1 platform, and this will be used as a baseline value for the discussion to follow.) This suggests a very fast and simple way of determining whether or not a cloud is present within a single infrared field of view. A look-up table is used to convert a microwave measurement of total water column to a predicted infrared clear-sky line depth. (The look-up table is based on climatological surface and atmospheric properties.) The observed line-depth is compared to the predicted clear-sky depth, and if they differ by more than 1 K a cloud detection flag is set to True.

To see what types of clouds are detectable by this line-depth threshold approach, Fig. 4 shows the change in depth from the clear-sky case, as a function of cloud height and amount in the Tropical atmosphere. (Cloud amount is measured by the effective cloud fraction: the product of the fractional area covered by clouds and the cloud emissivity.) The greater the cloud amount or the greater the cloud's altitude, the more it changes the line depth. In the case of a 1 K knowledge of the clear sky line depth, the region of parameter space in Fig. 4 above and to the right of the 1 K contour will be recognized as containing a cloud. For optically thick clouds (where cloud fraction equals the effective cloud fraction), any cloud more than 75 mbar from the surface is detectable if its areal coverage is at least 50%. At 100% coverage, even a cloud within a few tens of mbars of the surface is recognizable. Middle and high altitude clouds have a stronger signal than low ones, and their presence is easily detected even at fractions as low as 20%.

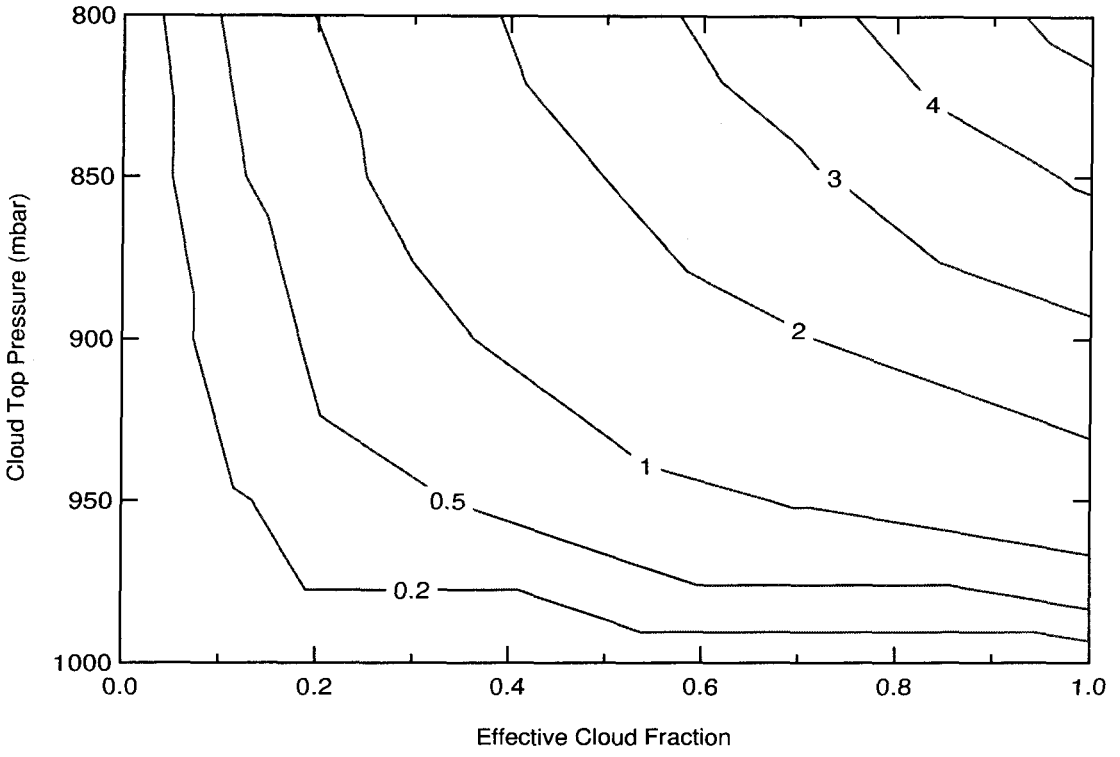

Figure 4: Contours of the difference between the clear-sky line depth and the cloudy line depth for the McClatchey Tropical atmosphere, as a function of cloud altitude and amount. The line used is the 1121.23 cm^{-1} water line, shown in Fig. 1. In these calculations, the clouds are assumed to be non-transmissive, and the Effective Cloud Fraction is the product of the cloud emissivity and the fractional area within the field-of-view covered by clouds. As cloud top pressure increases (moving upward on the graph), more of the water vapor is screened from our view and the clear/cloudy difference gets larger. Similarly, the greater the cloud fraction (moving to the right) the greater the difference.

Figure 5 is similar to Fig. 4, but cloud effects are shown for the 5 other McClatchey atmospheres. Results for the US Standard (water column 1.4 g cm^{-2}), Mid-Latitude Summer (water column 2.8 g cm^{-2}), and Sub-Arctic Summer (water column 2.0 g cm^{-2}) are quite similar to the Tropical case (water column 4.0 g cm^{-2}). For the two winter profiles, the line depth is much less sensitive to clouds. This is because the total water column in these cold atmospheres is quite small (0.8 g cm^{-2} at mid-latitudes, 0.4 in the arctic). In addition to a small water column, the Sub-Arctic Winter profile has a strong inversion, creating a region of negative contour values.

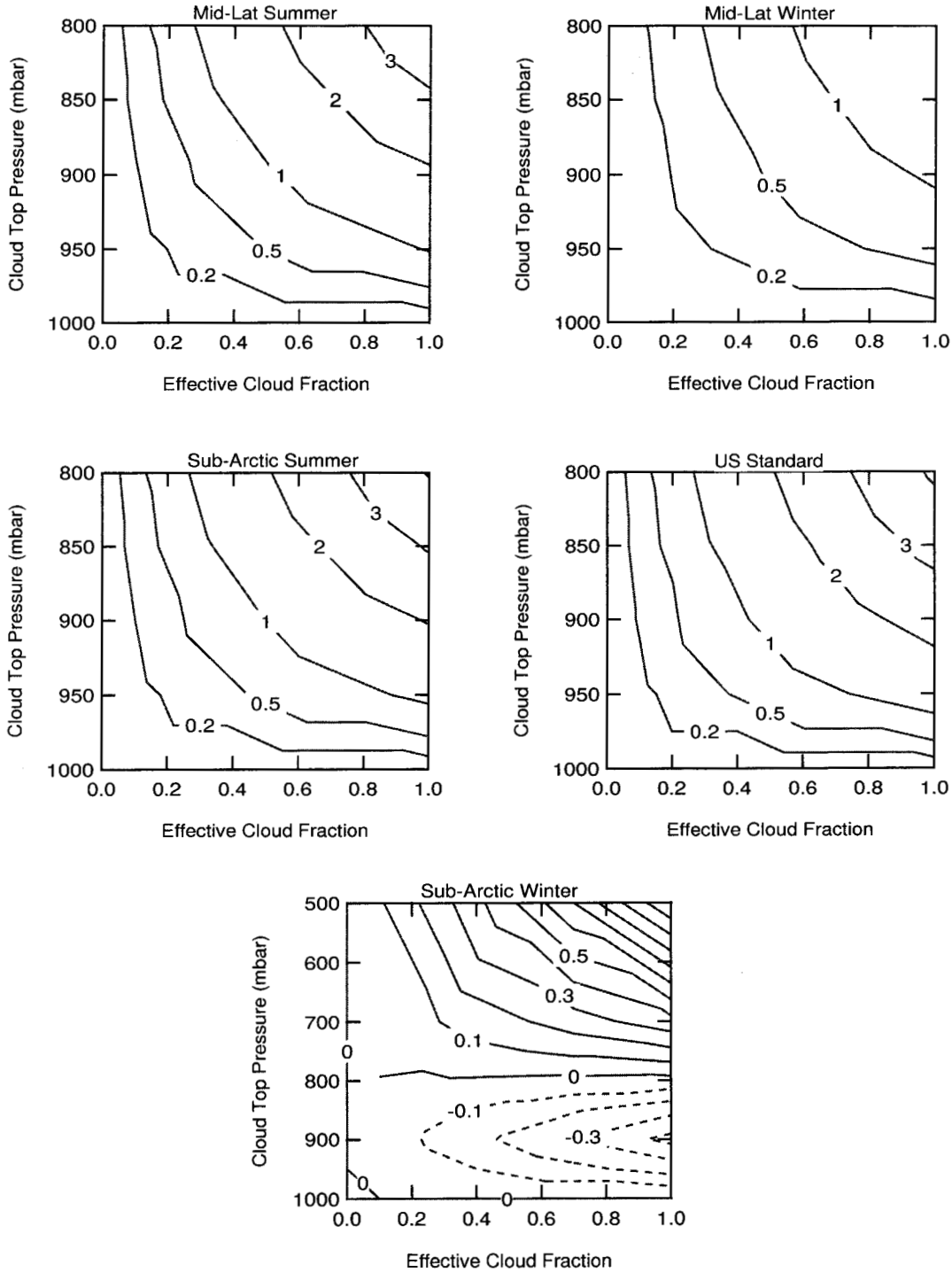

Figure 5: Same as Fig. 4, but for the 5 other McClatchey atmospheres. The Mid-Latitude Summer case is in the upper left, Mid-Latitude Winter in the upper right, Sub-Arctic Summer is middle left, and the US Standard Atmosphere is middle right. All these atmospheres yield similar results, with the magnitude of the signal determined by the total water column. The bottom panel is for the Sub-Arctic Winter profile. This last profile is unique in that it has a strong inversion layer that tops out near 800 mbar. This, combined with the extremely low water column (one tenth of the Tropical value), places additional structure in the contour field.

Figures 4 and 5 indicate that the cloud signal is strongest in moist atmospheres with high cloud fractions. This is precisely the situation in which traditional techniques are most likely to mistake low-cloud tops for the surface and thereby provide an erroneous retrieval. We conclude that this easy to compute cloud flag can be useful either as a pre-processing input into traditional atmospheric and surface retrieval algorithms, or as a quality flag to such retrievals.

3. Retrieving Cloud Height and Amount

The previous section has shown how observations of optically thin water vapor lines can be used to determine whether or not a single infrared FOV contains a cloud. A very simple and fast algorithm was presented, but one that does not return any physical properties of the cloud. In this section we discuss how, with some knowledge of vertical temperature and water vapor profiles, these lines can be used to retrieve low-cloud height and amount. We include an error analysis comparing our approach to traditional techniques, as was first reported in Hofstadter and Heidinger (1997). We then present some results from applying our algorithm to model data. In our analysis, we make the following assumptions:

- There is only one cloud layer in the FOV.
- Clouds are non-transmissive.
- Clouds are blackbodies.
- Atmospheric temperature and water vapor profiles are the same in both clear and cloudy regions within the FOV.

We find that, compared to traditional IR analysis, the line-depth technique is significantly more accurate in determining low-cloud properties in moist atmospheres. This conclusion should be valid even when the above assumptions are relaxed.

Let D_{obs} refer to an observed line depth, the radiance difference between a window frequency and a nearby, optically thin, line center. The field-of-view for this observation contains both clear and cloudy columns. Let D_{clr} and D_{cld} be the line depths that would be observed from hypothetical 100% clear and 100% cloudy FOV's. If N is the fraction of the FOV containing cloudy columns, these quantities are related by:

$$D_{obs} = D_{clr} + N\left(D_{cld} - D_{clr}\right). \tag{1}$$

Next, consider a spectrometer that simultaneously observes two of these weak water lines in the same FOV, referred to as lines i and j. We define a quantity called the "Z-function",

$$Z^{ij} = \frac{D^i_{obs} - D^i_{clr}}{D^j_{obs} - D^j_{clr}}, \tag{2}$$

where the superscripts indicate which optically thin line is being measured. Finally, by combining (1) and (2), we see that Z can also be expressed as

$$Z^{ij} = \frac{D^i_{cld} - D^i_{clr}}{D^j_{cld} - D^j_{clr}}. \tag{3}$$

If the temperature and water vapor profiles are known, D_{clr} can be calculated. Equation 2 then allows Z^{ij} to be determined. If the cloud layer is a non-transmissive blackbody, the line depth for a given weak water line and atmospheric profile is a function of cloud-top pressure only, $D_{cld} = D_{cld}(P_c)$. Equation 3 then expresses Z^{ij} as a function of cloud-top pressure only. This suggests the following scheme for retrieving cloud properties. First, temperature and vapor profiles are assumed based on climatology, microwave measurements, or traditional IR retrievals. From the assumed profiles, D_{clr} is calculated. Observations of the lines i and j then allow Z^{ij} to be determined from (2). Once Z^{ij} is known, (3) is inverted for the cloud top pressure, which also determines D^i_{cld} and D^j_{cld}. Finally, since all the D_x are now known, (1) can be solved for N. We thus have retrieved

values for the cloud height and amount. At the end of this section we present numerical examples of applying this approach.

The above approach is mathematically identical to traditional algorithms for retrieving cloud quantities, except that we have replaced absolute radiances with the differential quantity, D. In particular, our Z-function is analogous to the G-function discussed by Chahine (1970, 1974). The advantage to using our Z-function is that it is much less sensitive to uncertainties in the assumed temperature profile than is the G-function. This allows the cloud retrieval to be much more accurate. To see this, we can estimate the uncertainty in the retrieved cloud-top pressure, P_c, and cloud fraction, N. The two sources of error are measurement noise, which effects D_{obs}, and errors in the assumed profiles, which effect D_{clr} and D_{cld}. In the following, we use U_X to mean the uncertainty associated with parameter "X".

We can approximate the uncertainty in P_c by $U_{Pc} = \frac{dP_c}{dZ} U_Z$, with U_Z given by

$$U_{Z^{ij}} = \sqrt{\left[U_{D^i_{obs}} \frac{\partial Z^{ij}}{\partial D^i_{obs}}\right]^2 + \left[U_{D^j_{obs}} \frac{\partial Z^{ij}}{\partial D^j_{obs}}\right]^2 + \left[U_{D^i_{clr}} \frac{\partial Z^{ij}}{\partial D^i_{clr}}\right]^2 + \left[U_{D^j_{clr}} \frac{\partial Z^{ij}}{\partial D^j_{clr}}\right]^2}.$$

The above expression for U_Z assumes the four error terms on the right are uncorrelated. This is not strictly true since the terms in D^i_{clr} and D^j_{clr} both arise from errors in the assumed profiles. Nonetheless, the approximation should be valid to a factor of $\sim\sqrt{2}$.

Taking partial derivatives of (2) to determine the $\frac{\partial Z}{\partial D}$ terms leads to

$$U_{Pc} = \frac{\partial P_c}{\partial Z^{ij}} \frac{1}{D^j_{obs} - D^j_{clr}} \sqrt{\left(U^2_{D^i_{obs}} + U^2_{D^i_{clr}}\right) + \left(U^2_{D^j_{obs}} + U^2_{D^j_{clr}}\right)\left(\frac{D^i_{obs} - D^i_{clr}}{D^j_{obs} - D^j_{clr}}\right)^2}. \quad (4)$$

Similarly, we can use (1) to determine the uncertainty in the retrieved cloud amount:

$$U_N = \frac{1}{D_{cld} - D_{clr}} \sqrt{U^2_{D_{obs}} + U^2_{D_{clr}}\left[\frac{D_{obs} - D_{cld}}{D_{cld} - D_{clr}}\right]^2 + U^2_{D_{cld}}\left[\frac{D_{obs} - D_{clr}}{D_{cld} - D_{clr}}\right]^2}. \quad (5)$$

In (5), the i or j superscript is dropped because either spectral line may be used. These uncertainty estimates assume observations of only a single line-pair for U_{Pc}, and a single line for U_N.

To use Eqs. 4 and 5 we must have estimates of all quantities on the right-hand side, all of which are functions of the water lines used and the observed atmosphere. We have chosen six representative lines for study. They are shown in Table II, with frequency and intensity information taken from the HITRAN data base (Rothman *et al.* 1992). There are two relatively strong lines (designated "S"), two relatively weak (designated "W"), and two intermediate ones ("I"). These 6 lines yield 15 usable values of Z^{ij}, where we note that Z^{ij} contains the same information as Z^{ji}.

Table II
Weak Water Lines Used in This Study

Designation	Frequency (cm^{-1})	Intensity (cm mol^{-1} at 296 K)	Clear Sky Line Depth in Tropical Atmosphere (K)	(mW m^{-2} $ster^{-1}$ cm)
S1	1121.23	5.40E-23	10.4	13.20
S2	871.25	1.97E-23	6.2	9.88
I1	1091.20	2.75E-23	5.3	6.83
I2	881.08	2.41E-24	2.0	3.49
W1	1085.44	2.29E-24	1.2	1.76
W2	875.95	2.80E-25	0.2	0.49

For a given atmosphere, cloud structure, and line pair, D_{clr}, D_{cld}, D_{obs}, Z^{ij}, and $\frac{\partial P_c}{\partial Z^{ij}}$ are calculated using a radiative transfer forward model developed by the AIRS Science Team. This leaves U_{Dobs}, U_{Dclr}, and U_{Dcld} to be determined. Current estimates place the AIRS noise equivalent temperature (NEΔT) in the 0.08 to 0.13 K range for frequencies near 1000 cm^{-1}, yielding a U_{Dobs} of ~0.17 mW m^{-2} $ster^{-1}$ cm. The estimate of U_{Dclr} chosen is based on the performance of AIRS atmospheric retrievals (using traditional algorithms) on a simulated data set. The simulation covers both land and ocean footprints containing variable amounts of two cloud-layers—though no cloud is at a pressure greater than 500 mbar. (Low clouds are excluded so that we may assess the limiting case of what can be achieved with an optimal cloud retrieval algorithm.) U_{Dclr} is taken to be the average of the residuals between the line-depths for the simulated clear-sky spectrum and the retrieved clear-sky spectrum. The last parameter we wish to estimate is U_{Dcld}. In the presence of a good cloud retrieval algorithm, we would expect U_{Dcld} to be of the same order as U_{Dclr}. For our purposes, we therefore assume $U_{Dcld} = U_{Dclr}$. Table IIIa lists the values used for each of these parameters.

We now have all the information needed to estimate the accuracy of our new retrieval algorithm using Eqs. 4 and 5. For comparison, we would like to make similar estimates for the traditional IR sounding technique. To do this, we note that Eqs. 1 through 5 are still valid if the line depth, D, is replaced by an absolute radiance measurement, I. The Z-Function then becomes the standard G-Function (Chahine 1970). We chose several frequencies for use in the G-Function: 733, 749, and 765 cm^{-1} are in the 15 micron CO_2 band, and 902 cm^{-1} is in a window region. These frequencies include ones that have been used in traditional cloud retrievals, and ones that have weighting functions that peak at or near the surface (Chahine 1974, Wielicki and Coakley 1981). For these calculations, a spectral resolution of 6 cm^{-1} is used, to avoid resolving fine spectral structure and to reduce the nominal AIRS noise level by a factor of 3. The resulting values of U_{Iobs}, U_{Iclr}, and U_{Icld} (determined in the same manner as the line-depth parameters described in the previous paragraph) are given in Table IIIb.

Table IIIa
Line Depth Uncertainty in mW m^{-2} $ster^{-1}$ cm

Line	U_{Dobs}	U_{Dclr} and U_{Dcld}
S1	0.17	0.4
S2	0.17	0.4
I1	0.17	0.2
I2	0.17	0.4
W1	0.17	0.05
W2	0.17	0.01

Table IIIb
Radiance Uncertainty in mW m^{-2} $ster^{-1}$ cm

Frequency (cm^{-1})	U_{Iobs}	U_{Iclr} and U_{Icld}
733	0.06	0.5
749	0.06	0.9
765	0.06	1.6
902	0.06	1.5

Calculations of U_{Pc} and U_N have been carried out for the 6 McClatchey atmospheres discussed in Section 2, for cloud tops in the 950 to 500 mbar range, and cloud fractions varying from 10% to 100%. The uncertainties are calculated using all combinations of frequencies listed in Table III, and the line pair yielding the smallest error for any situation is reported as the uncertainty for that situation. For example, with a cloud at 900 mbar covering 70% of the FOV in the McClatchey tropical profile, the uncertainty in retrieved P_c using the water line technique is ~240 mbar, and U_N is 9%. Under the same conditions the traditional retrieval technique has an uncertainty in P_c of ~330 mbar, and an uncertainty in cloud fraction of 18%. For reasons discussed below, the important quantity to keep in mind is the relative uncertainty of the two retrievals: the new line depth technique is significantly more accurate in this situation.

The reasons to de-emphasize the absolute values calculated by Eqs. 4 and 5 are that first, they do not account for improvements in accuracy allowed by simultaneously fitting more than one line-pair, and second, their derivation and the estimates of U_{Dclr} and U_{Dcld} contain assumptions that make the results only approximate. Because the same assumptions go into the error estimates for both techniques, however, the relative errors should be more reliable. In Table IV, we therefore compare the accuracy of the two techniques by showing the percent improvement in going from the traditional to the line-depth technique, where percent improvement is defined as

$$\frac{\text{Uncertainty(Traditional)} - \text{Uncertainty(LineDepth)}}{\text{Uncertainty(Traditional)}}.$$

Note that a negative improvement means the traditional technique is superior. Another advantage to quoting percent improvement is that the values are insensitive to cloud fraction, allowing Table IV to apply to all values of N from ~10% to ~90%. In the completely clear or completely cloudy cases, U_{Pc} is unchanged from Table IV, but the performance of the new technique in determining N is better than is indicated in the table.

Table IV
Percent Improvement in the Uncertainty

True P_C	Tropical Atmosphere		Mid-Latitude Summer		U.S. Standard Atmosphere 1962	
(mbar)	U_{Pc} (mbar)	U_N	U_{Pc} (mbar)	U_N	U_{Pc} (mbar)	U_N
950	40	55	15	40	-65	15
900	30	50	0	40	-90	10
850	10	45	-15	30	-120	5
800	-5	40	-30	25	-150	-5

Table IV points out that for low clouds in moist atmospheres, the line depth technique is superior. As the atmosphere becomes drier, or clouds move higher (above most of the water vapor), the traditional approach becomes superior. Note, however, that even when cloud altitude cannot be retrieved, the new technique can still accurately set a true/false cloud flag as discussed in Section 2.

As a test of retrieving cloud height with the proposed technique, we applied the "Z-function" algorithm just described to simulated AIRS data. Based on the performance of the prototype AIRS retrieval software, we assume that the tropospheric temperature profile is known to 1 K rms in 1 km thick layers, with a bias temperature of ±0.2 K. We also assume that the water vapor amount in such layers is known to 10% rms with a bias of ±5%. We applied these assumed errors as noise to the McClatchey tropical atmosphere, and then generated simulated AIRS radiances for both the exact and the noise added atmospheric profiles. In the simulations we included one optically thick cloud layer, with cloud-top altitude ranging from 950 to 500 mbar, and cloud fraction varying from 0 to 100%. We then used the algorithm described following (3), with the noise-added profiles being used to calculate D_{clr} and the dependence of Z on P_c, and the noise-free atmospheric profiles used to generate the "observed" values, D_{obs} and Z^{ij}. P_c is retrieved by simultaneously matching all 15 values of Z^{ij} in a least-squares sense. In this situation, we find that cloud-top altitude can be determined with an rms error of 55 mbar for clouds between 950 and 800 mbar and having an effective cloud fraction ≥70%. We also find that the True/False cloud test described in Section 2 could reliably detect any cloud fraction greater than 10%. (This performance is much better than that predicted in Section 2 because here we allow information from the full IR-microwave retrieval to constrain the water vapor profile, while previously we assumed only the microwave total water column was available.) These limited retrieval tests do not fully characterize the proposed technique, but they do attest to its utility under some conditions. Future work will more rigorously explore the effects of incorporating the line-depth technique into a complete atmospheric retrieval scheme.

4. Summary

We have found that high spectral resolution infrared observations can make use of optically thin water vapor lines to probe clouds. With knowledge of the total water column (which is easily provided by microwave sounders), a fast and simple test can set a true/false flag for the presence of clouds. This cloud test works on a single infrared footprint (unlike some current techniques which require multiple fields-of-view), and in a moist atmosphere can recognize even extremely low clouds (within 50 mbar of the surface). This is an important tool for infrared sounding because traditional techniques can mistake a warm, low cloud for the surface. We have also demonstrated that by incorporating these lines into retrieval algorithms, one can expect an improved determination of low-cloud altitude and amount in moist atmospheres. This technique will be used with AIRS data to give us a more complete picture of the three-dimensional distribution of clouds in Earth's atmosphere.

Acknowledgments

The authors wish to thank Moustafa Chahine and Robert Haskins for advice and support in carrying out this research, Sung-Yung Lee and the AIRS Project for providing the radiative transfer forward model, and Eric Fetzer for access to his radiosonde data base. This work was carried out at the Jet Propulsion Laboratory, California Institute of Technology, under contract with the National Aeronautics and Space Agency.

REFERENCES

Aumann, H.H., and R.J. Pagano, 1994. Atmospheric Infrared Sounder on the Earth Observing System. *Opt. Eng.* **33**, 776–784.

Chahine, M.T., 1974: Remote Sounding of Cloud Atmospheres. I. The Single Cloud Layer. *J. Atm. Sci.* **31**, 323–243.

Chahine, M.T., 1970: Inverse Problems in Radiative Transfer: Determination of Atmospheric Parameters. *J. Atm. Sci.* **27**, 960–967.

Chahine, M.T., 1968: Determination of the Temperature Profile in an Atmosphere from its Outgoing Radiance. *J. Opt. Soc. Am.* **58**, 1634-1637.

Hofstadter, M.D., and A. Heidinger, 1997: Infrared Low-Cloud Detection. *Optical Remote Sensing of the Atmosphere, OSA Technical Digest Series*, **5**, 100–102. (Conference Proceedings, February 1997, Santa Fe.)

McClatchey, R.A., R.W. Fenn, J.E.A. Selby, F.E. Volz, and J.S. Garing, 1972: *Optical Properties of the Atmosphere*. 3rd ed. AFCGRL-72-0497, 113 pp.

O'Brien, D.M., S.A. English, and G.A. Da Costa, 1997: High-Precision, High-Resolution Measurements of Absorption in the Oxygen A-Band. *J. Atm. Ocean. Tech.* **14**, 105–119.

Rothman, L.S., R.R. Gamache, R.H. Tipping, C.P. Rinsland, M.A.H. Smith, D. Chris Benner, V. Malathy Devi, J.M. Flaud, C. Camy-Peyret, A. Perrin, A. Goldman, S.T. Massie, L.R. Brown, and R.A. Toth, 1992. The HITRAN Molecular Database: Editions of 1991 and 1992. *J. Quant. Spectrosc. Radiat. Transfer* **48**, 469-507.

Smith, W.L., 1968: An Improved Method for Calculating Tropospheric Temperature and Moisture from Satellite Radiometer Measurements. *Mon. Wea. Rev.* **96**, 387–396.

Wielicki, B.A., and J.A. Coakley, 1981. Cloud Retrieval Using Infrared Sounder Data: Error Analysis. *Jour. App. Met.* **20**, 157–169.